Commun. Comput. Phys.
doi: 10.4208/cicp.190313.090913a

Vol. **15**, No. 3, pp. 776-796
March 2014

A Penalty Optimization Algorithm for Eigenmode Optimization Problem Using Sensitivity Analysis

Zhengfang Zhang[1,*], Weifeng Chen[2] and Xiaoliang Cheng[3]

[1] *College of Science, Hangzhou Dianzi University, Hangzhou 310018, P.R. China.*
[2] *School of Information, Zhejiang University of Finance and Economics, Hangzhou 310018, P.R. China.*
[3] *Department of Mathematics, Zhejiang University, Hangzhou 310027, P.R. China.*

Received 19 March 2013; Accepted (in revised version) 9 September 2013

Communicated by Bo Li

Available online 3 December 2013

Abstract. This paper investigates the eigenmode optimization problem governed by the scalar Helmholtz equation in continuum system in which the computed eigenmode approaches the prescribed eigenmode in the whole domain. The first variation for the eigenmode optimization problem is evaluated by the quadratic penalty method, the adjoint variable method, and the formula based on sensitivity analysis. A penalty optimization algorithm is proposed, in which the density evolution is accomplished by introducing an artificial time term and solving an additional ordinary differential equation. The validity of the presented algorithm is confirmed by numerical results of the first and second eigenmode optimizations in $1D$ and $2D$ problems.

AMS subject classifications: 35Q60, 49R05, 65F15, 65F18, 90C31

Key words: Sensitivity analysis, eigenmode optimization problem, finite element method, penalty method.

1 Introduction

To investigate the structural dynamics characteristics of mechanical systems, the use of modal analysis is widely applied. The modal pairs consist of eigenfrequencies and eigenmodes are used to identify the cause of vibrational problems. By making use of the eigenpairs, one can evaluate the change of dynamical properties when mass and/or stiffness is added or subtracted without changing the structure.

*Corresponding author. *Email addresses:* zhengfangzhang@hdu.edu.cn (Z. Zhang), chenweifeng@cad.zju.edu.cn (W. Chen), xiaoliangcheng@zju.edu.cn (X. Cheng)

The vibration control at low frequency is an important research field [25, 26]. To design devices with the specified dynamic structural optimization, various numerical optimization algorithms are established with respect to the structure design variables such as size, shape and topology [1, 8, 19, 30]. For avoidance of resonance, one effective method is to maximize the lowest eigenfrequency to determine the shape of the vibrating membrane composed of materials with different densities [6, 15, 41]. Osher and Santosa [28] solve the model problem by the level set method [29], combining the variational level set method [42] and the projection gradient method [31]. A monotonic algorithm [40], based on resorting order, can efficiently deal with the eigenvalue optimizations of multi-density materials. Another kind of eigenvalue optimization problems arises from a large class of problems in the field of boundary control or reinforcement [5, 33]. Cox and Uhlig [7] analyze the existence and convergence of the eigenvalue boundary optimization, establish the pointwise optimal condition, and test a pair of numerical methods. Zhang and Cheng [39] propose a boundary piecewise constant level set method to parameterize the boundary condition and convert the eigenvalue optimization problem to rely on a parameter instead of the boundary geometry, which generalizes the classical piecewise constant level set method [34].

Eigenmode optimization, another branch of vibration optimization problems, is of great importance. Typical examples are mechanical resonators that are used as sensors, oscillators, filters and actuators. In this type of resonator, the eigenmode that dominates the shape of deformation against the external periodic load is an important design factor in addition to the resonance frequency. One popular technique is the topology optimization [8,19,21,23], based on homogenization theory proposed by Bendsøe and Kikuchi [2]. In this technique, the material distribution is formulated with parameters in periodic microstructures. Another currently used method is the SIMP (solid isotropic material with penalization) method [9, 16, 18, 36]. The basic idea of SIMP is taking use of a fictitious isotropic material whose elasticity tensor is expressed by an exponent parameter and assumed to be a function of penalized material density. However, these topology optimization methods cause numerical problems such as checkerboard patterns, grey scales and artificial parameter dependance.

Sensitivity analysis is a fundamental tool for the optimization problems in both the discrete form and the continuum form. For the eigenmode optimization problem, some researchers use eigenmode sensitivity analysis of matrices, which are derived by the finite element method (FEM) discretization of original continuum problem [10, 22, 38]. In [21], vibrating structures with specified eigenfrequencies and eigenmode shapes are investigated. Maeda et al. propose a new topology optimization method based on homogenization theory and derive the sensitivity of the eigenvalue and eigenmode with respect to design variable after FEM discretization is performed. In continuum form, to the best of the authors' knowledge, sensitivity analysis for eigenmode optimization problem are reported by [17,35]. In [17], Inzarulfaisham and Azegami evaluate the shape gradient for the boundary shape optimization problem with optimality conditions obtained by the adjoint variable method, the Lagrange multiplier method and the formula for the mate-

rial derivative. However, the derivative of the eigenmode optimization problem requires higher order eigenfrequencies and eigenmodes, which imply the increasing computational cost. Takezawa and Kitamura [35] obtain the derivative of the objective functional including the k-th eigenmode and the adjoint variable, which avoids the computation of higher order eigenfrequencies and eigenmodes. In their numerical experiments, the eigenmode approach the prescribed eigenmode convergently, but the optimal distribution of the design variable is a little jagged.

Taking advantage of the sensitivity analysis in the continuum form, we obtain the derivative of the objective functional including the k-th eigenvalue and the k-th eigenmode and the adjoint variable, which excludes higher order eigenfrequencies and eigenmodes. We further calculate the first variation of the k-th eigenvalue and avoid to calculate the gradient of the k-th eigenmode and the adjoint variable in the derivative of the objective functional. The quadratic penalty method [24] is applied to treat the lower bound constraint and convert the constrained optimization problem to an unconstrained one. The first variation of the penalty term with respect to the density function is also calculated. The density function evolves in a dynamic way, where an artificial time term is introduced and an ordinary differential equation (ODE) with respect to the time is constructed. A third-order Runge-Kutta method [12, 13] is applied to solve the ODE. Based on the above strategies, we propose a penalty optimization algorithm. In our numerical experiments, the first and second eigenmode optimization problems in $1D$ and $2D$ domains are considered. The penalty optimization algorithm performs effectively and efficiently to match the target eigenmode without or with lower bound constraint. Moreover, the finial distribution of the density function is smooth.

This paper is organized as follows. In Section 2, the eigenmode optimization problem is described. The first variation of the eigenmode optimization problem is derived in Section 3. In Section 4, we propose a penalty optimization algorithm. In Section 5, we present the numerical results for the first two least eigenmodes optimization problems without and with constraints in $1D$ and $2D$ domains. The last section gives some concluding remarks.

2 Problem statement

Consider the wave equation

$$\rho(x)\frac{\partial^2 U(x,t)}{\partial t^2} = \Delta U(x,t), \quad \text{in } \Omega\times[0,T], \tag{2.1a}$$

$$U(x,t) = 0, \quad \text{on } \partial\Omega\times[0,T], \tag{2.1b}$$

where Ω is a smooth, bounded and connected subset of R^n $(n=1,2)$, $\partial\Omega$ is the boundary of Ω and $\rho(x)$ is the density of string or membrane with positive lower bound ρ_1 and upper bound ρ_2. Set $U(x,t)=e^{-i\omega t}u(x)$, where ω is the frequency and $u(x)$ is the amplitude.

Then Eqs. (2.1a) and (2.1b) are converted to the scalar Helmholtz equation

$$-\Delta u = \lambda \rho u, \quad \text{in } \Omega, \tag{2.2a}$$
$$u = 0, \quad \text{on } \partial\Omega, \tag{2.2b}$$

where λ is eigenvalue of $-\Delta$, satisfying $\lambda = \omega^2$. Using integration by parts, we have the weak formulation

$$\int_\Omega \nabla u \cdot \nabla v dx = \lambda \int_\Omega \rho u v dx, \quad \forall v \in H_0^1(\Omega), \tag{2.3}$$

where $H_0^1(\Omega)$ denotes Sobolev space of square integrable, until the first order derivative, functions defined in Ω with zero boundary value on $\partial\Omega$. Subsequently, the k-th least eigenvalue λ_k is obtained by the Rayleigh quotient [14]

$$\lambda_k(\rho) = \min_{u \in A_k} \frac{\int_\Omega |\nabla u|^2 dx}{\int_\Omega \rho u^2 dx}, \tag{2.4}$$

where

$$A_k = \left\{ u \in H_0^1(\Omega) : \int_\Omega u^2 dx = 1, \int_\Omega u u_l dx = 0, \, l = 1, 2, \cdots, k-1 \right\} \tag{2.5}$$

and u_l is the l-th eigenmode corresponding to the l-th eigenvalue. The minimizer in (2.4) is the k-th eigenmode u_k and the k-th least eigenvalue λ_k is assumed to be simple.

Given a target eigenmode $\hat{u}_k$, one need to match the k-th eigenmode u_k to the target eigenmode while the eigenvalue λ_k is constrained to be greater than Λ. The eigenmode optimization problem can be formulated as the minimization problem of the squared error integral

$$\min_\rho F(\rho) = \int_\Omega (u_k - \hat{u}_k)^2 dx, \tag{2.6}$$

such that

$$\lambda_k \geq \Lambda, \tag{2.7a}$$
$$0 < \rho_1 \leq \rho(x) \leq \rho_2. \tag{2.7b}$$

3 Sensitivity analysis

We attempt to solve the optimization problem (2.6)-(2.7) using gradient-type algorithms. Therefore, the gradient of eigenmode optimization problem with respect to density function ρ is of practical interest. To do so, we first establish the differentiability of the k-th eigenpair $u_k(\rho)$ and $\lambda_k(\rho)$, the solutions to (2.2a) and (2.2b), by taking the first variation on both sides of Eqs. (2.2a) and (2.2b) and defining the sensitivity problem:

$$-\Delta(u_k'(\rho)\theta) = \lambda_k'(\rho)\theta\rho u_k + \lambda_k \theta u_k + \lambda_k \rho u_k'(\rho)\theta, \quad \text{in } \Omega, \tag{3.1a}$$
$$u_k'(\rho)\theta = 0, \quad \text{on } \partial\Omega, \tag{3.1b}$$

where $u_k'(\rho)\theta$ and $\lambda_k'(\rho)\theta$ represent the first variations of $u_k(\rho)$ and $\lambda_k(\rho)$ with respect to ρ in direction θ, respectively. The first variation of a functional $J(y)$ is defined as the linear functional $J'(y)$ mapping the function h to

$$J'(y)h=\lim_{\varepsilon\to 0}\frac{J(y+\varepsilon h)-J(y)}{\varepsilon},$$

where y and h are functions, and ε is a scalar [11]. The adjoint problem is introduced by

$$-\Delta w-\lambda_k\rho w=u_k-\hat{u}_k, \quad \text{in } \Omega, \tag{3.2a}$$
$$w=0, \quad \text{on } \partial\Omega, \tag{3.2b}$$

where w is the adjoint variable.

Using integration by parts, we have the weak formulations for (3.1a) and (3.1b)

$$\int_\Omega \nabla(u_k'(\rho)\theta)\nabla v dx=\lambda_k'(\rho)\theta\int_\Omega \rho u_k v dx+\lambda_k\int_\Omega \theta u_k v dx + \lambda_k\int_\Omega \rho u_k'(\rho)\theta v dx, \quad \forall v\in H_0^1(\Omega) \tag{3.3}$$

and for (3.2a) and (3.2b)

$$\int_\Omega \nabla w\nabla p dx-\lambda_k\int_\Omega \rho w p dx=\int_\Omega (u_k-\hat{u}_k)p dx, \quad \forall p\in H_0^1(\Omega). \tag{3.4}$$

Set $v=w$ in (3.3) and $p=u_k'(\rho)\theta$ in (3.4), then one can obtain

$$\int_\Omega (u_k-\hat{u}_k)u_k'(\rho)\theta dx=\lambda_k'(\rho)\theta\int_\Omega \rho u_k w dx+\lambda_k\int_\Omega \theta u_k w dx. \tag{3.5}$$

Again, set $v=u_k$ in (3.3) and apply the integration by parts, then we have

$$-\int_\Omega u_k'(\rho)\theta\Delta u_k dx=\lambda_k'(\rho)\theta\int_\Omega \rho u_k^2 dx+\lambda_k\int_\Omega \theta u_k^2 dx+\lambda_k\int_\Omega u_k'(\rho)\theta\rho u_k dx. \tag{3.6}$$

Since the eigenpair (λ_k,u_k) satisfies equation (2.2a), the left term and the third term on the right side in (3.6) can be eliminated and (3.6) is simplified by

$$\lambda_k'(\rho)\theta\int_\Omega \rho u_k^2 dx+\lambda_k\int_\Omega \theta u_k^2 dx=0. \tag{3.7}$$

That is,

$$\lambda_k'(\rho)\theta=-\frac{\lambda_k\int_\Omega \theta u_k^2 dx}{\int_\Omega \rho u_k^2 dx}. \tag{3.8}$$

Substituting (3.8) into (3.5), we obtain

$$\begin{aligned}\int_\Omega (u_k-\hat{u}_k)u_k'(\rho)\theta dx &= -\frac{\lambda_k\int_\Omega \theta u_k^2 dx}{\int_\Omega \rho u_k^2 dx}\int_\Omega \rho u_k w dx+\lambda_k\int_\Omega \theta u_k w dx\\ &= -\lambda_k\int_\Omega \Big[\frac{\int_\Omega \rho u_k w dx}{\int_\Omega \rho u_k^2 dx}u_k^2-u_k w\Big]\theta dx. \end{aligned} \tag{3.9}$$

Taking the first variation of the objective optimization functional $F(\rho)$ in (2.6) with respect to ρ in direction θ and using (3.9), we obtain

$$\begin{aligned}F'(\rho)\theta &= 2\int_\Omega (u_k-\hat{u}_k)u_k'(\rho)\theta dx\\ &= -2\lambda_k\int_\Omega \Big[\frac{\int_\Omega \rho u_k w dx}{\int_\Omega \rho u_k^2 dx}u_k^2-u_k w\Big]\theta dx. \end{aligned} \tag{3.10}$$

Thus, the derivative of $F(\rho)$ with respect to ρ is evaluated by

$$F'(\rho) = -2\lambda_k\Big[\frac{\int_\Omega \rho u_k w dx}{\int_\Omega \rho u_k^2 dx}u_k^2-u_k w\Big]. \tag{3.11}$$

4 Algorithms

For the minimization problem (2.6) with constraints (2.7a) and (2.7b), one can use the penalty method [3, 24, 32] and change the constrained optimization problem into an unconstrained one. There are two wildly used penalty methods : the quadratic penalty method and exact penalty method (see [24] and the references therein). In our algorithm, we use the quadratic penalty method. To deal with the inequality constraint (2.7a), we define the penalty function by

$$Q(\rho;\mu) = F(\rho)+\frac{1}{\mu}\Big[\max(\Lambda-\lambda_k(\rho),0)\Big]^2, \tag{4.1}$$

where $\mu>0$ is the penalty parameter. To determine the derivative of $Q(\rho;\mu)$ with respect to ρ, we first obtain the derivative of $\lambda_k(\rho)$ with respect to ρ from (3.8) by

$$\lambda_k'(\rho) = -\frac{\lambda_k u_k^2}{\int_\Omega \rho u_k^2 dx}. \tag{4.2}$$

Combining (3.11) with (4.2), the derivative of $Q(\rho;\mu)$ with respect to ρ is calculated by

$$\frac{dQ(\rho;\mu)}{d\rho} = \begin{cases} -2\lambda_k\Big[\dfrac{\int_\Omega \rho u_k w dx}{\int_\Omega \rho u_k^2 dx}u_k^2-u_k w+\dfrac{1}{\mu}\dfrac{(\lambda_k-\Lambda)u_k^2}{\int_\Omega \rho u_k^2 dx}\Big], & \lambda_k<\Lambda,\\ -2\lambda_k\Big[\dfrac{\int_\Omega \rho u_k w dx}{\int_\Omega \rho u_k^2 dx}u_k^2-u_k w\Big], & \lambda_k\geq\Lambda. \end{cases} \tag{4.3}$$

Considering the stationary condition for (4.1), it is necessary to satisfy

$$\frac{dQ(\rho;\mu)}{d\rho}=0. \tag{4.4}$$

However, directly solving Eq. (4.4) is not an easy work. We introduce an artificial time term and solve the following ordinary differential equation to the steady state [20, 34]

$$\rho_t+\frac{dQ(\rho;\mu)}{d\rho}=0, \tag{4.5a}$$

$$\rho(0)=\rho^0. \tag{4.5b}$$

In this paper, we solve this ODE by a third-order Runge-Kutta scheme (cf. [12, 13] and references therein):

$$\rho^{(1)}=\rho^k-\Delta t^k\frac{dQ}{d\rho}(\rho^k;\mu^k), \tag{4.6a}$$

$$\rho^{(2)}=\frac{3}{4}\rho^k+\frac{1}{4}\rho^{(1)}-\frac{1}{4}\Delta t^k\frac{dQ}{d\rho}(\rho^{(1)};\mu^k), \tag{4.6b}$$

$$\rho^{k+1}=\frac{1}{3}\rho^k+\frac{2}{3}\rho^{(2)}-\frac{2}{3}\Delta t^k\frac{dQ}{d\rho}(\rho^{(2)};\mu^k), \tag{4.6c}$$

where Δt^k is the time step, which should be small enough to keep the iteration stability of the scheme. It is heuristic to limit the time step to satisfy the following condition

$$\Delta t^k<h\Big/\max_{x\in\Omega}\Big|\frac{dQ}{d\rho}(\rho^k(x);\mu^k)\Big|, \tag{4.7}$$

where h is the fineness of the spatial discretization (see [4, 27]). The penalty parameter is updated adaptively, $\mu^{k+1}\in(0,\mu^k)$ (see [24]), based on the difficulty of minimizing the penalty function at each iteration. If minimization of $Q(\rho;\mu^k)$ proves to be expensive for some k, μ^{k+1} is chosen to be only modestly smaller than μ^k; for instance $\mu^{k+1}=0.9\mu^k$. When calculation of the minimizer of $Q(\rho;\mu^k)$ is cheap, a more ambitious reduction can be chosen, for instance $\mu^{k+1}=0.1\mu^k$. In our algorithm, we set μ^k to be a constant.

For the constraint (2.7b), we define a project to let the density function ρ in the interval $[\rho_1,\rho_2]$, that is,

$$P_{[\rho_1,\rho_2]}\rho=\begin{cases}\rho_1, & \rho<\rho_1,\\ \rho, & \rho_1\le\rho\le\rho_2,\\ \rho_2, & \rho>\rho_2.\end{cases} \tag{4.8}$$

Now, the penalty optimization algorithm is presented as follows.

Algorithm 4.1. Initialize ρ^0 in the whole domain. The constants ρ_1, ρ_2, Λ, μ and $\hat{u}_k$ are given.

Do for $m=0,1,2,\cdots$

STEP 1. Compute (λ_k^m, u_k^m) by (2.2a) with boundary condition (2.2b).

STEP 2. Compute w^m, the solution of adjoint problem (3.2a) and (3.2b) with λ_k^m, u_k^m and ρ^m.

STEP 3. Compute ρ^*, the solution of (4.5a) and (4.5b) with $\rho(0)=\rho^m$, by the third-order Runge-Kutta scheme in (4.6a)-(4.6c).

STEP 4. Update ρ^{m+1} by the projection defined in (4.8)

$$\rho^{m+1}=P_{[\rho_1,\rho_2]}\rho^*.$$

STEP 5. Check the convergence, if convergence, stop. Otherwise, $m=m+1$ and go to STEP 1.

Remark 4.1. In STEP 3, we use the third-order Runge-Kutta scheme in (4.6a)-(4.6c). For the condition (4.7), we set the time step

$$\Delta t^k=\alpha h\Big/\max_{x\in\Omega}\Big|\frac{dQ}{d\rho}(\rho^k(x);\mu)\Big|,\quad \alpha\in(0,1).$$

5 Numerical results

In this section, we present some numerical results on experiments of penalty optimization algorithm for the eigenmode optimization problem (2.6)-(2.7) in both 1D and 2D domains. We consider the 1D domain $\Omega=[0,1]$ and partition it by 100 line elements. In 2D model, the domain is a rectangle, that is, $\Omega=[0,1]\times[0,0.8]$ and we partition it by 50×40 square elements. To solve Helmholtz equation (2.2a) and (2.2b), we use finite element method with piecewise linear bases. The penalty optimization algorithm runs in MATLAB codes conducted by ourselves and the discretized Helmholtz equation is solved by the ***eigs*** function found in MATLAB [37].

For the 1D problem, the target eigenmodes are set to be the following two cases: For the first eigenmode optimization problem

$$\hat{u}_1=0.8304\times e^x\sin(\pi x),\quad 0\le x\le 1; \tag{5.1}$$

For the second eigenmode optimization problem

$$\hat{u}_2=\begin{cases}0.8304\times e^{2x}\sin(2\pi x), & 0\le x<0.5,\\ 0.8304\times e^{2-2x}\sin(2\pi x), & 0.5\le x\le 1.\end{cases} \tag{5.2}$$

For the 2D problem, the target eigenmodes are set to be the following two cases: For the first eigenmode optimization problem

$$\hat{u}_1=0.8619\times e^x e^y\sin(\pi x)\sin(1.25\pi y),\quad 0\le x\le 1,\ 0\le y\le 0.8; \tag{5.3}$$

For the second eigenmode optimization problem

$$\hat{u}_2=\begin{cases}1.3129\times e^{2x}\sin(2\pi x)\sin(1.25\pi y), & 0\le x<0.5,\ 0\le y\le 0.8,\\ 1.3129\times e^{2-2x}\sin(2\pi x)\sin(1.25\pi y), & 0.5\le x\le 1,\ 0\le y\le 0.8.\end{cases} \tag{5.4}$$

The coefficients are added to normalize $\hat{u}_k$, that is, $\int_\Omega \hat{u}_k^2 dx=1$, $k=1,2$. These functions are plotted in Fig. 1. In all our numerical examples, we set $\rho_1=1$ and $\rho_2=10$.

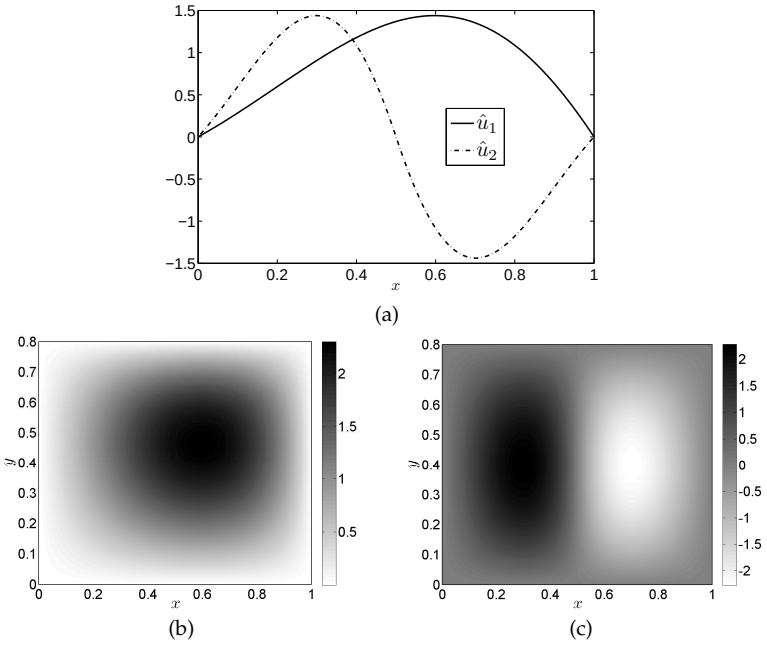

Figure 1: The target eigenmodes. (a) The first eigenmode $\hat{u}_1$ and the second eigenmode $\hat{u}_2$ in $1D$ problem. (b) The first eigenmode $\hat{u}_1$ in $2D$ problem. (c) The second eigenmode $\hat{u}_2$ in $2D$ problem.

5.1 Examples without lower bound Λ

We first study the numerical examples for the first and second eigenmodes matching problems in $1D$ and $2D$ domains without lower bound Λ. Therefore, the penalty terms in (4.1) and (4.3) are omitted. Algorithm 4.1 is adjusted accordingly.

Fig. 2 illustrates the evolution of density distribution and comparison of the computed first eigenmode with the target first eigenmode in initial state and after 50, 100, 200, 500, 1000 iterations. Starting from the initial density distribution $\rho^0 = 2$, as shown in Fig. 2(a), the first eigenmode has a great deviation from the target eigenmode. As iterations process, density distribution varies according to the shape of the target eigenmode. Higher density materials are distributed in right-side interval $(0.6,1)$. After 1000 iterations, as illustrated in Fig. 2(f), the optimal eigenmode u_1 (solid curve) achieves good approximation to the target eigenmode $\hat{u}_1$ (dash curve). The iteration history of the objective functional $F(\rho)$ and the squared error integral of the first eigenmode u_1 and the target eigenmode $\hat{u}_1$ are plotted in Fig. 3. The evolution of the least eigenvalue λ_1 is shown in Fig. 3 as well. We obtain the optimal $F(\rho) = 4.9316E\text{-}4$ and $\lambda_1 = 4.1971$. Compared with the numerical results in [35], where the optimal $F(\rho) = 3.524E\text{-}3$ and $\lambda_1 = 4.535$ with the same mesh size, the penalty optimization algorithm obtains 7 times smaller minimized functional $F(\rho)$. Thus, it is 7 times closer to the target first eigenmode for the optimal computed first eigenmode by the penalty optimization algorithm than by the method in [35]. Moreover, the distribution of the density ρ by the penalty optimization algorithm

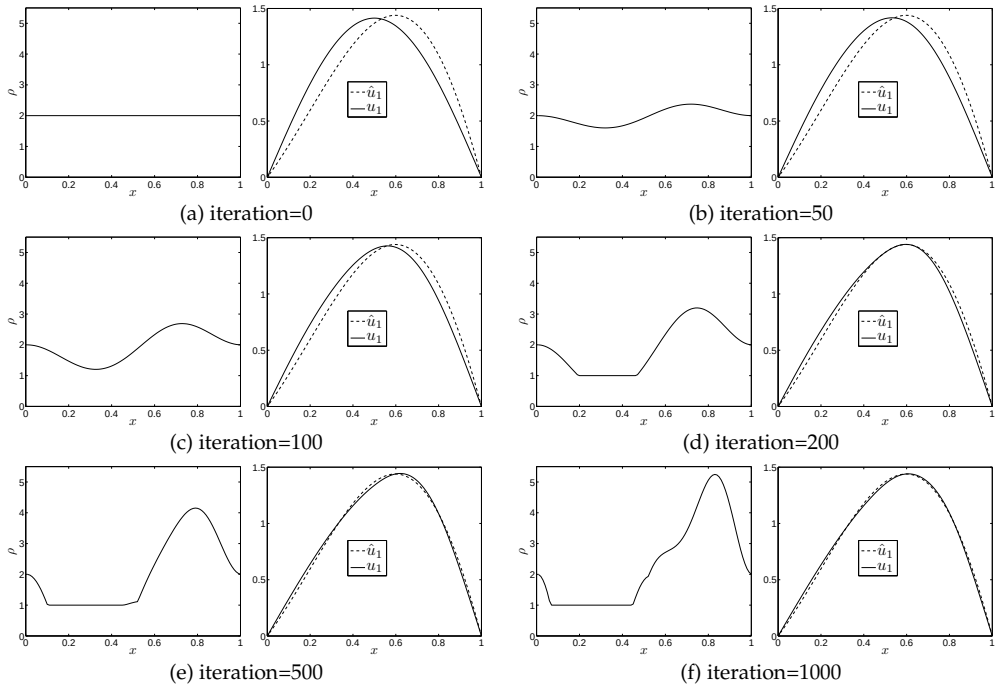

Figure 2: The evolution profiles of density distribution and the first eigenmode distribution in $1D$ problem. (a) The initial density distribution (left) and the first eigenmodes (right), where the solid curve is the first eigenmode u_1 and the dash curve is the target eigenmode $\hat{u}_1$. (b)-(f) are density distributions (left) and the first eigenmodes (right) after 50, 100, 200, 500 and 1000 iterations.

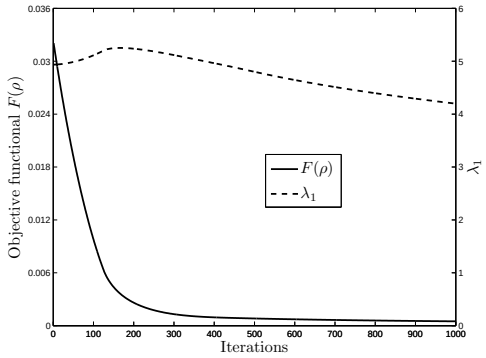

Figure 3: The iteration histories of the objective functional $F(\rho)$ and the first eigenvalue λ_1 in $1D$ problem, corresponding to evolutions of the density distribution in Fig. 2.

is smoother than the distribution of c, the reciprocal of the density (see Fig. 7(a) in [35]).

Another initial density distribution is conceived and illustrated in Fig. 4(a). That is,

$$\rho^0(x)=\begin{cases} 4, & 0.2\le x\le 0.4, \\ 1, & 0\le x<0.2,\ 0.4<x\le 1. \end{cases} \tag{5.5}$$

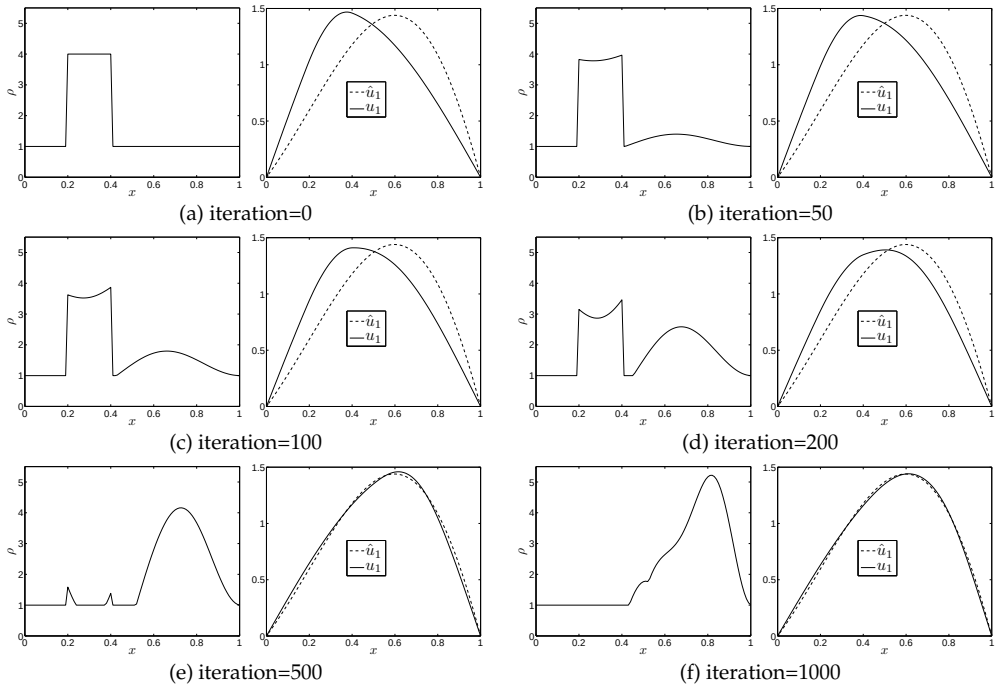

Figure 4: The evolution profiles of density distribution and the first eigenmode distribution in $1D$ problem. (a) The initial density distribution (left) and the first eigenmodes (right), where the solid curve is the first eigenmode u_1 and the dash curve is the target eigenmode $\hat{u}_1$. (b)-(f) are density distributions (left) and the first eigenmodes (right) after 50, 100, 200, 500 and 1000 iterations.

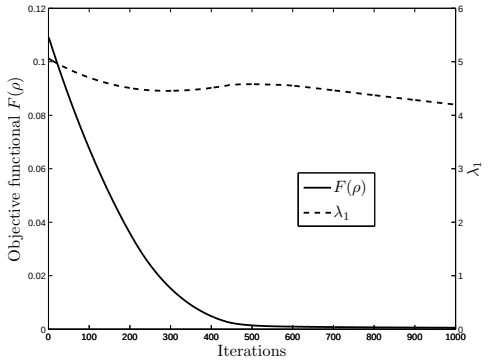

Figure 5: The iteration histories of the objective functional $F(\rho)$ and the first eigenvalue λ_1 in $1D$ problem, corresponding to evolutions of the density distribution in Fig. 4.

The high density materials are distributed in the left-side interval $[0.2,0.4]$, which is opposite to the optimal density distribution as shown in Fig. 2(f). Therefore, the computed first eigenmode u_1 has more deviation from the target eigenmode $\hat{u}_1$ than the first case as illustrated in Fig. 2(a). The evolutions of the density distribution and the first eigenmode u_1 are shown in Fig. 4, after 50, 100, 200, 500 and 1000 iterations. The density in

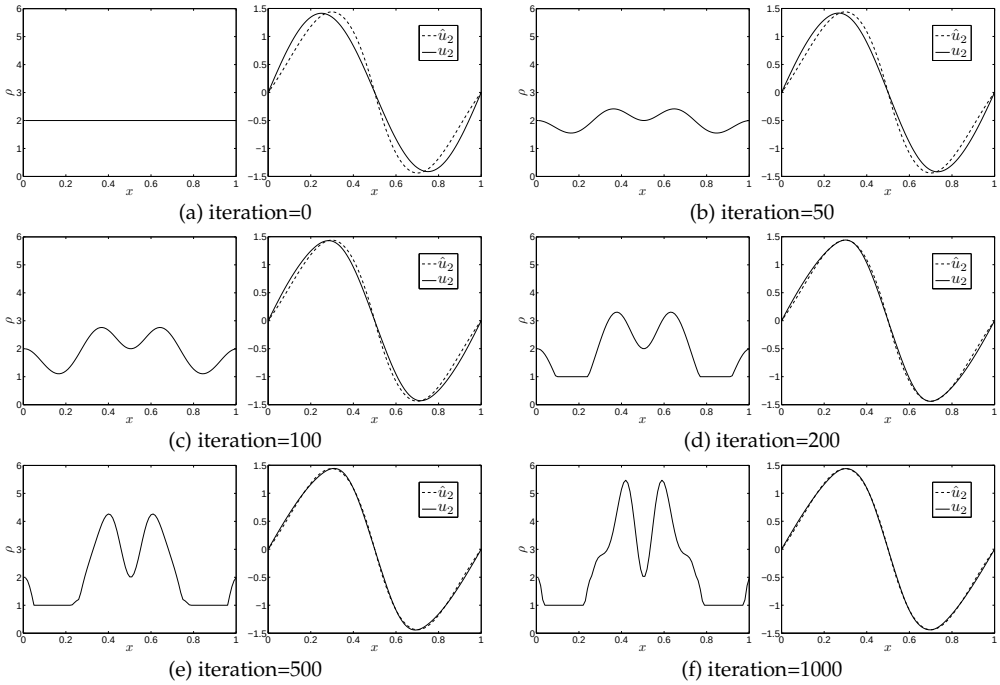

Figure 6: The evolution profiles of density distribution and the second eigenmode distribution in $1D$ problem. (a) The initial density distribution (left) and the second eigenmodes (right), where the solid curve is the second eigenmode u_2 and the dash curve is the target eigenmode $\hat{u}_2$. (b)-(f) are density distributions (left) and the second eigenmodes (right) after 50, 100, 200, 500 and 1000 iterations.

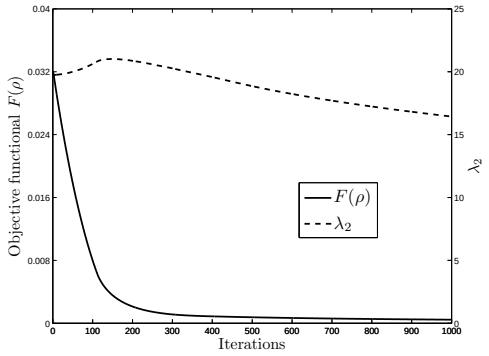

Figure 7: The iteration histories of the objective functional $F(\rho)$ and the second eigenvalue λ_2 in $1D$ problem.

the left-side interval $[0.2,0.4]$ is cutting down, while in the right-side interval $[0.4,0.9]$, the density is enlarging. The computed first eigenmode u_1 is increasingly close to the target first eigenmode $\hat{u}_1$. The optimal $F(\rho) = 5.5651E\text{-}4$ and $\lambda_1 = 4.1975$ after 1000 iterations, which are in accord with the optimal results of the first density initialization. Fig. 5 illustrates the iteration histories of the objective functional $F(\rho)$ and the first eigenvalue λ_1 corresponding to evolutions of the density distribution in Fig. 4.

With different initial density distributions, however, the penalty optimization algorithm obtains the similar optimal density distribution except for the subdomains close to both ends. The density differences at both ends are caused by the homogenous Dirichlet boundary condition (2.2b), which makes the derivatives in (4.3) become zero and keeps the density function fixed at both ends. However, these little differences do not affect the convergence of the computed eigenmode to the target eigenmode. Therefore, the initial density is uniformly $\rho^0 = 2$ in the following numerical examples, unless otherwise specified.

For the second eigenmode optimization in $1D$ problem, the penalty optimization algorithm also performs successfully. The evolution profiles of density distribution and the second eigenmode distribution are illustrated in Fig. 6. Fig. 7 illustrates the evolution of the objective functional $F(\rho)$ and the second least eigenvalue λ_2. After 1000 iterations, we obtain the optimal objective functional $F(\rho) = 4.5694E\text{-}4$ and the second least eigenvalue $\lambda_2 = 16.4333$, corresponding to the density distribution and eigenmode shown in Fig. 6(f).

For $2D$ optimization problems, the density and eigenmode distribution vary similarly to the $1D$ optimization problems. In Fig. 8, the evolution profiles of density distribution and the first eigenmode distribution are illustrated. According to the shape of the target eigenmode shown in Fig. 1(b), higher density materials are concentrated in the upper right corner of the rectangle (see Fig. 8(f)). The iteration histories of objective functional

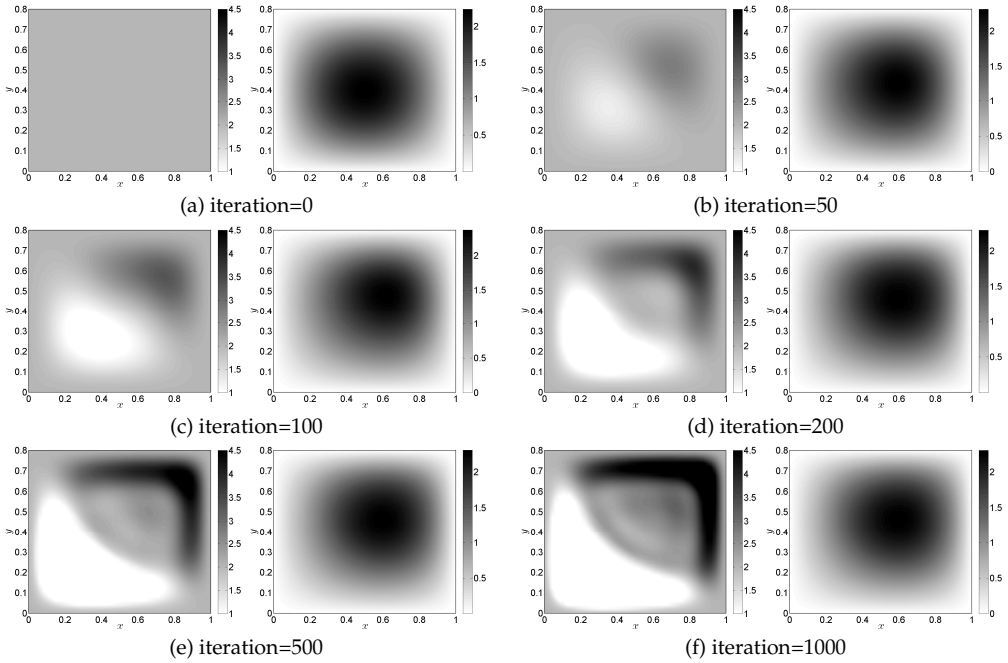

(a) iteration=0 (b) iteration=50

(c) iteration=100 (d) iteration=200

(e) iteration=500 (f) iteration=1000

Figure 8: The evolution profiles of density distribution and the first eigenmode distribution in $2D$ problem. (a) The initial density distribution (left) and the initial first eigenmode (right). (b)-(f) are density distributions (left) and the first eigenmode distributions (right) after 50, 100, 200, 500 and 1000 iterations.

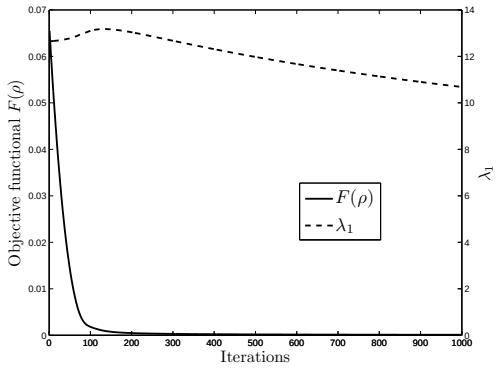

Figure 9: The iteration histories of the objective functional $F(\rho)$ and the first eigenvalue λ_1 in $2D$ problem.

$F(\rho)$ and the first eigenvalue λ_1 in $2D$ problem are shown in Fig. 9. The optimal objective functional $F(\rho)=1.0056E$-4, which is 78 times smaller than the optimal objective functional $F(\rho)=7.905E$-3 in [35]. The final first eigenvalue $\lambda_1=10.6807$, a little smaller than the optimal first eigenvalue $\lambda_1=12.055$ in [35]. The results of the second eigenmode optimization problem are shown in Fig. 10 and Fig. 11 with the optimal objective functional $F(\rho)=1.0821E$-3 and $\lambda_2=28.7245$.

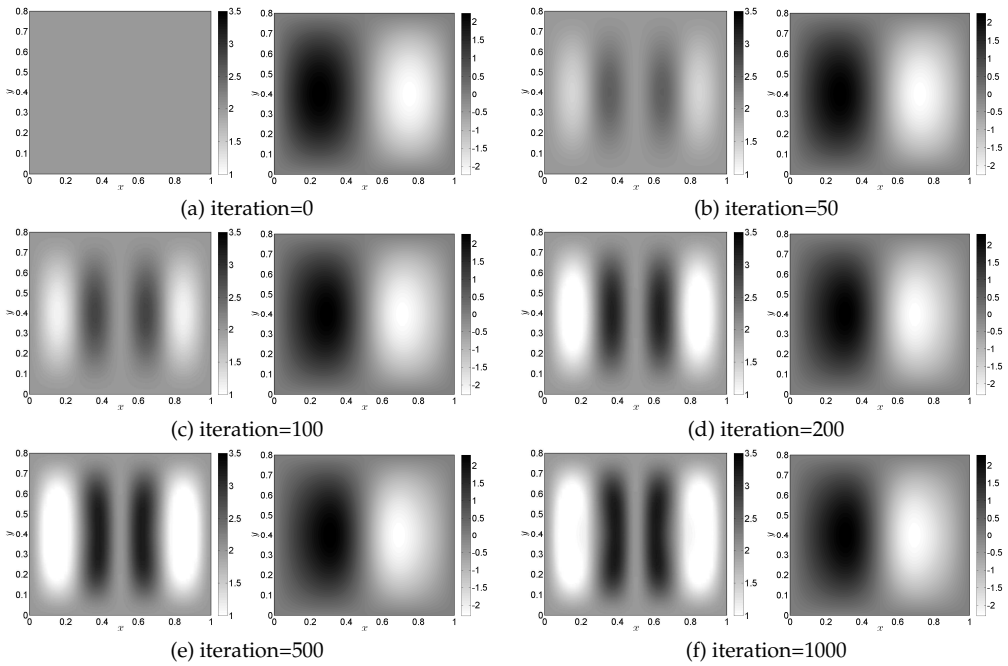

(a) iteration=0 (b) iteration=50

(c) iteration=100 (d) iteration=200

(e) iteration=500 (f) iteration=1000

Figure 10: The evolution profiles of density distribution and the second eigenmode distribution in $2D$ problem. (a) The initial density distribution (left) and the initial second eigenmode (right). (b)-(f) are density distributions (left) and the second eigenmode distributions (right) after 50, 100, 200, 500 and 1000 iterations.

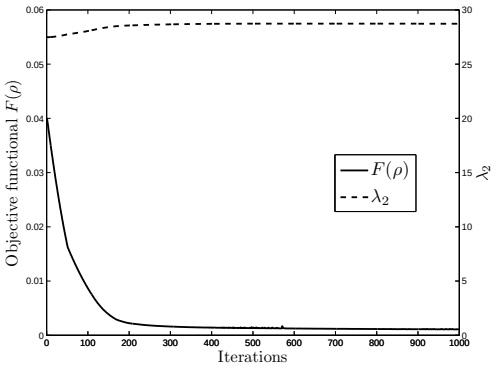

Figure 11: The iteration histories of the objective functional $F(\rho)$ and the second eigenvalue λ_2 in $2D$ problem.

5.2 Examples with lower bound Λ

In this section, we set lower bounds for eigenvalues. We investigate the first eigenmode matching problem in $1D$ and $2D$ under the constraint that the first eigenvalue should be larger than a given number Λ. The lower bounds of the first eigenvalue are chosen as 5, 6, 7, 8 for $1D$ problem and 14, 16, 18, 20 for $2D$ problem. The penalty parameters are set to be $\mu=0.01$ in $1D$ problem and $\mu=0.1$ in $2D$ problem.

Fig. 12 illustrates the optimal results for first eigenmode optimization in $1D$ problem with lower bounds 5, 6, 7 and 8. One can observe that the larger the value of the lower bound is, the more deviation from the target eigenmode the optimal eigenmode has (see Fig. 12(b), (d), (f), (h)). Moreover, to have a larger eigenvalue, the string must be as light as possible. The increase of the density is weakened because the lower bound becoming larger (see Fig. 12(a), (c), (e), (g)). Compared with the jagged distribution of c (see Fig. 11) in [35], the reciprocal of the density, the penalty optimization algorithm obtains quite smooth distributions of the optimal density ρ under the lower bound constraints for the least eigenvalue.

In Table 1, the optimal objective functional $F(\rho)$ and the least eigenvalue λ_1 are listed, for the first eigenmode optimization in $1D$ problem without or with lower bound con-

Table 1: Comparisons of penalty optimization algorithm (POA) and method in [35] for the first eigenmode optimization in 1D problem with 100 elements.

	POA		method in [35]	
Λ	$F(\rho)$	λ_1	$F(\rho)$	λ_1
None	$4.9316E-4$	4.1971	$3.524E-3$	4.535
5	$7.3989E-4$	5.0064	null	null
6	$1.4330E-3$	6.0462	$4.931E-3$	6.314
7	$3.0823E-3$	7.0109	$1.035E-2$	7.033
8	$7.5381E-3$	8.0131	$2.600E-2$	7.981

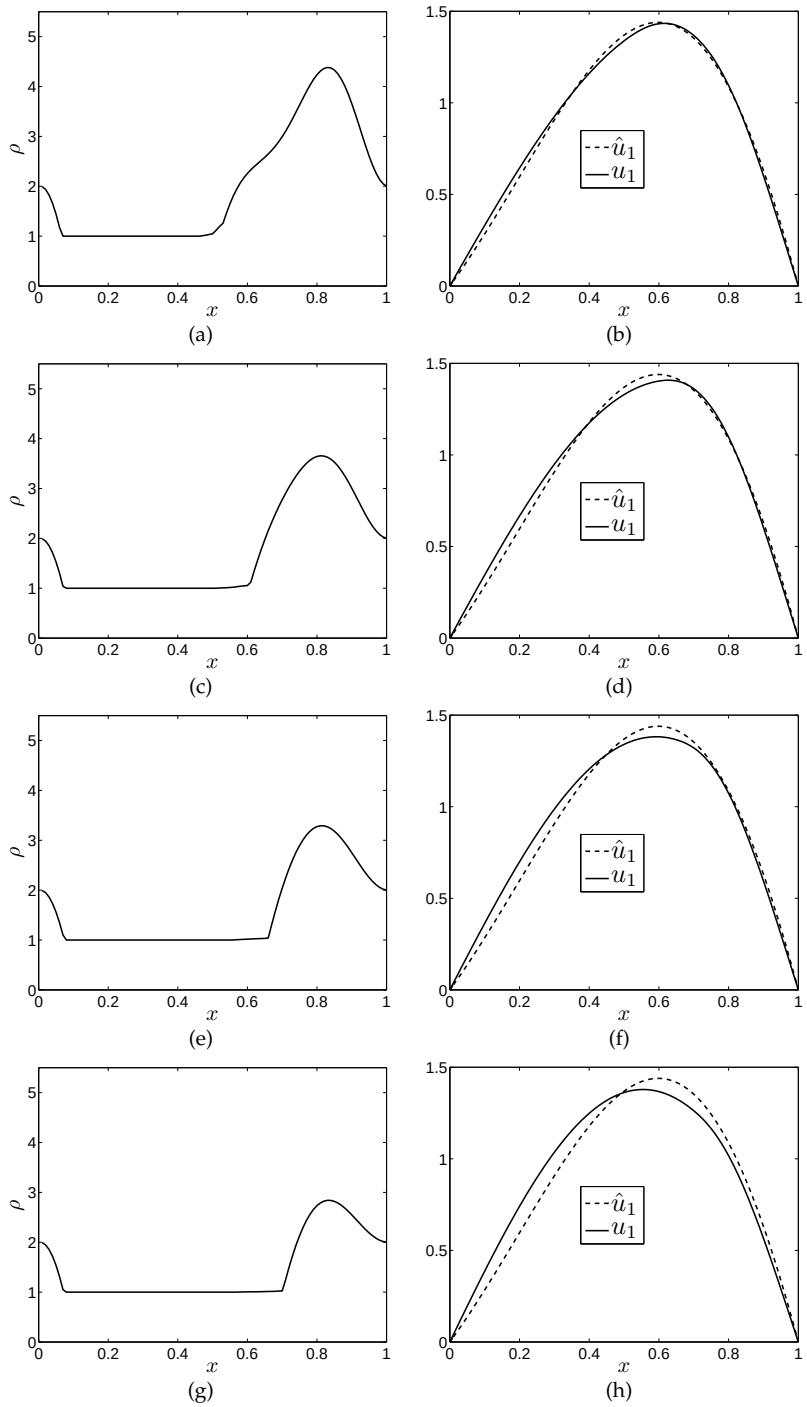

Figure 12: Optimal results for the first eigenmode optimization in $1D$ problem. (a), (c), (e), (g) Optimal distributions of density ρ with lower bound 5, 6, 7 and 8. (b), (d), (f), (h) Comparisons of optimal eigenmode u_1 and target eigenmode $\hat{u}_1$ with lower bound 5, 6, 7 and 8.

straints 5, 6, 7 and 8. The inequality constraints on the first eigenvalue are successfully satisfied, as shown in Table 1. However, the optimal objective functional $F(\rho)$ becomes larger because the constraint leads to a smaller solution space. The same phenomenon is illustrated in [35]. As listed in Table 1, the penalty optimization algorithm obtains almost 3.5 times smaller optimal objective functional $F(\rho)$ than the method in [35], satisfying the lower bound constraint for the least eigenvalue. Furthermore, the optimal least eigenvalues λ_1 are closer to their lower bounds by the penalty optimization algorithm than by the method in [35], to obtain a more minimized objective functional $F(\rho)$.

The numerical results of the first eigenmode optimization problem in $2D$ domain under lower bound constraint are shown in Fig. 13 and Table 2. In Fig. 13, lower density materials are distributed in the upper right corner of the rectangle domain as the lower bound increasing. The deviation of the optimal eigenmode u_1 from the target eigenmode $\hat{u}_1$ is observed by comparing the eigenmode distribution in Fig. 13(b), (d), (f), (h) and in Fig. 1(b). Compared with the optimal distribution of c in [35] (see Fig. 12), the penalty optimization algorithm obtains smoother optimal distribution of density. The quantitative comparisons of the penalty optimization algorithm and the method in [35] are illustrated in Table 2. Although the lower bound constraints 14, 16, 18 and 20 are satisfied, the optimal objective functional $F(\rho)$ is becoming larger when the lower bound is increasing. The penalty optimization algorithm obtains 25, 15, 9, 8 times smaller optimal objective functional $F(\rho)$ than the method in [35], under the lower bound constraints 14, 16, 18, 20, respectively.

Table 2: Comparisons of penalty optimization algorithm (POA) and method in [35] for the first eigenmode optimization in 2D problem with 40×50 elements.

	POA		method in [35]	
Λ	$F(\rho)$	λ_1	$F(\rho)$	λ_1
None	$1.0056E-4$	10.6807	$7.905E-3$	12.055
14	$3.1487E-4$	14.0815	$7.912E-3$	14.860
16	$6.6264E-4$	16.0122	$9.633E-3$	16.047
18	$1.7069E-3$	18.0567	$1.572E-2$	18.000
20	$4.3957E-3$	19.9882	$3.455E-2$	20.000

Our numerical tests are performed in Matlab 7.11.0 (R2010b) environment on a desktop PC equipped with Intel Core i5-2320 CPU at 3.00GHz and 8 GB of RAM memory. The total CPU times (in seconds) for eigenmode optimization in 1D and 2D problems without or with constraints are shown in Table 3. The total 1000 iterations of penalty optimization algorithm cost CPU time of around 42 seconds for the first and second eigenmode optimization in 1D problems with 100 elements. In 2D eigenmode optimization problems with 40×50 elements, the total 1000 iterations of penalty optimization algorithm cost CPU time of around 304 seconds. Furthermore, the optimization problems with constraints take a little more CPU times than the unconstrained ones in 1D and 2D problems.

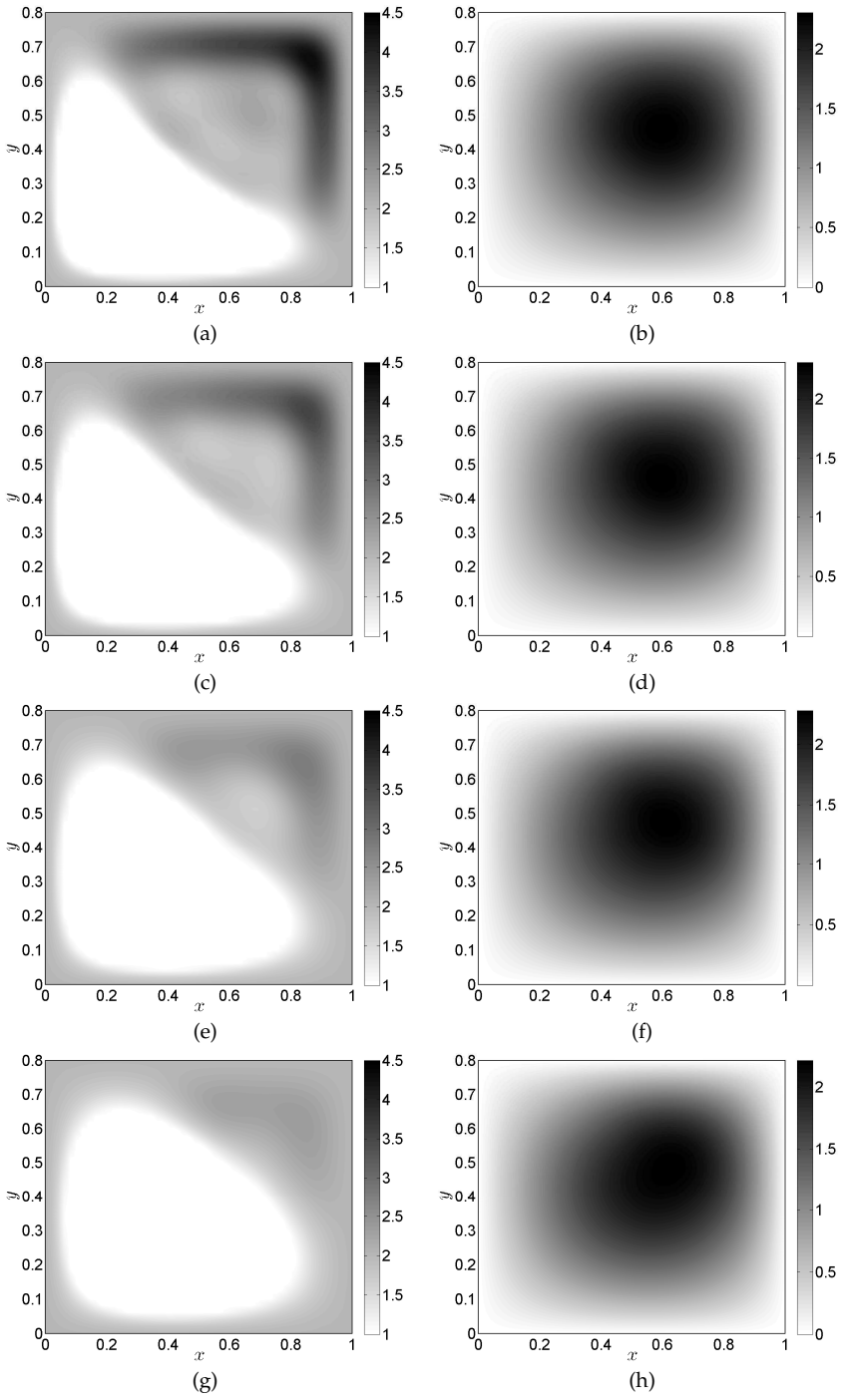

Figure 13: Optimal results for the first eigenmode optimization in $2D$ problem. (a), (c), (e), (g) Optimal distributions of density ρ with lower bound 14, 16, 18 and 20. (b), (d), (f), (h) Optimal distributions of first eigenmode u_1 with lower bound 14, 16, 18 and 20.

Table 3: The total CPU times (in seconds) for eigenmode optimization in 1D and 2D problems.

eigenmode optimization	1D		2D	
	Λ	CPU time (s)	Λ	CPU time (s)
$\min \int_\Omega (u_1 - \hat{u}_1)^2 dx$	None	41.454	None	303.470
	5	42.122	14	303.345
	6	41.955	16	303.072
	7	42.138	18	304.791
	8	42.169	20	306.175
$\min \int_\Omega (u_2 - \hat{u}_2)^2 dx$	None	42.721	None	304.352

6 Conclusion

This paper presents a penalty optimization algorithm for solving the eigenmode optimization problem in which the eigenmode shape approaches the prescribed eigenmode shape while the eigenvalue is constrained to be greater than Λ. We derive the first variation of the eigenvalue and eigenmode with respect to the density function. Thus the derivative of the objective functional is obtained, which is including current eigenvalue and eigenmode and adjoint variable. We avoid the calculation of the gradient of the current eigenmode and adjoint variable, and exclude the higher order eigenfrequencies and eigenmodes in the derivative of the eigenmode optimization problem. For the density evolution, we introduce an artificial time term and solve an ODE by a third-order Runge-Kutta scheme. The scalar Helmholtz equation and the adjoint problem are solved by finite element method. The first two eigenmodes matching problems in $1D$ and $2D$ domains are considered in numerical experiments. We observe that penalty optimization algorithm is effective to minimize the objective functional without or with lower bound constraint and the optimal density distribution is smooth. Since the penalty optimization algorithm is not restricted to $1D$ and $2D$ cases, it can be extended to $3D$ case. In addition, we expect the penalty optimization algorithm and sensitivity analysis to solve eigenmode optimization problems governed by vector Helmholtz equation.

Acknowledgments

This research is supported by National Natural Science Foundation of China (Nos. 11201106 and 61303134), Natural Science Foundation of Zhejiang Province, China (No. LQ12A01001) and Key Project of the Major Research Plan of NSFC (No. 91130004).

References

[1] G. Allaire, S. Aubry, and F. Jouve, Eigenfrequency optimization in optimal design, Comput. Methods Appl. Mech. Engrg., 190 (2001), pp. 3565–3579.

[2] M. P. Bendsøe and N. Kikuchi, Generating optimal topologies in structural design using a homogenization method, Comput. Methods Appl. Mech. Engrg., 71 (1988), pp. 197–224.
[3] S. Brenner, F. Li, and L. Sung, A locally divergence-free interior penalty method for two-dimensional curl-curl problems, SIAM J. Numer. Anal., 46 (2008), pp. 1190–1211.
[4] M. Burger, B. Hackl, and W. Ring, Incorporating topological derivatives into level set methods, J. Comput. Phys., 194 (2004), pp. 344–362.
[5] L. Cot, J. Raymond, and J. Vancostenoble, Exact controllability of an aeroacoustic model with a Neumann and a Dirichlet boundary control, SIAM J. Control. Optim., 48 (2009), pp. 1489–1518.
[6] S. Cox and J. McLaughlin, Extremal eigenvalue problems for composite membranes, I, Appl. Math. Opt., 22 (1990), pp. 153–167.
[7] S. Cox and P. Uhlig, Where best to hold a drum fast, SIAM J. Optim., 9 (1999), pp. 948–964.
[8] A. Díaaz and N. Kikuchi, Solutions to shape and topology eigenvalue optimization problems using a homogenization method, Int. J. Numer. Meth. Eng., 35 (1992), pp. 1487–1502.
[9] J. Du and N. Olhoff, Topological design of freely vibrating continuum structures for maximum values of simple and multiple eigenfrequencies and frequency gaps, Struct. Multidisc. Optim., 34 (2007), pp. 91–110.
[10] R. L. Fox and M. P. Kapoor, Rates of change of eigenvalues and eigenvectors, AIAA J., 6 (1968), pp. 2426–2429.
[11] M. Giaquinta and S. Hildebrandt, Calculus of Variations I, Springer, Berlin, 2004.
[12] S. Gottlieb and C. Shu, Total variation diminishing Runge-Kutta schemes, Math. Comput., 67 (1998), pp. 73–85.
[13] S. Gottlieb, C. Shu, and E. Tadmor, Strong stability-preserving high-order time discretization methods, SIAM Rev., 43 (2001), pp. 89–112.
[14] S. Gould, Variational Methods for Eigenvalue Problems: An Introduction to the Methods of Rayleigh, Ritz, Weinstein, and Aronszajn, Dover Publications, New York, 1957.
[15] E. Haber, A multilevel, level-set method for optimizing eigenvalues in shape design problems, J. Comput. Phys., 198 (2004), pp. 518–534.
[16] W. He, D. Bindel, and S. Govindjee, Topology optimization in micromechanical resonator design, Optim. Eng., 13 (2012), pp. 271–292.
[17] A. Inzarulfaisham and H. Azegami, Solution to boundary shape optimization problem of linear elastic continua with prescribed natural vibration mode shapes, Struct. Multidisc. Optim., 27 (2004), pp. 210–217.
[18] J. S. Jensen and N. L. Pedersen, On maximal eigenfrequency separation in two-material structures: the 1d and 2d scalar cases, J. Sound Vib., 289 (2006), pp. 967–986.
[19] T. Kim and Y. Kim, Mac-based mode-tracking in structural topology optimization, Comput. Struct., 74 (2000), pp. 375–383.
[20] H. Li and X. Tai, Piecewise constant level set method for interface problems, Int. Series Numer. Math., 154 (2007), pp. 307–316.
[21] Y. Maeda, S. Nishiwaki, K. Izui, M. Yoshimura, K. Matsui, and K. Terada, Structural topology optimization of vibrating structures with specified eigenfrequencies and eigenmode shapes, Int. J. Numer. Meth. Eng., 67 (2006), pp. 597–628.
[22] R. B. Nelson, Simplified calculation of eigenvector derivatives, AIAA J., 14 (1976), pp. 1201–1205.
[23] S. Nishiwaki, K. Saitou, S. Min, and N. Kikuchi, Topological design considering flexibility under periodic loads, Struct. Multidisc. Optim., 19 (2000), pp. 4–16.
[24] J. Nocedal and S. Wright, Numerical Optimization, Springer, New York, 1999.

[25] N. Olhoff, Maximizing higher order eigenfrequencies of beams with constraints on the design geometry, J. Struct. Mech., 5 (1977), pp. 107–134.
[26] N. Olhoff and G. Rozvany, Optimal grillage layout for given natural frequency, J. Eng. Mech. Div., 108 (1982), pp. 971–975.
[27] S. Osher and R. Fedkiw, Level Set Methods and Dynamic Implicit Surfaces, Springer, New York, 2002.
[28] S. Osher and F. Santosa, Level set methods for optimization problems involving geometry and constraints: I. Frequencies of a two-density inhomogeneous drum, J. Comput. Phys., 171 (2001), pp. 272–288.
[29] S. Osher and J. Sethian, Fronts propagating with curvature-dependent speed: algorithms based on Hamilton-Jacobi formulations, J. Comput. Phys., 79 (1988), pp. 12–49.
[30] N. Pedersen, Maximization of eigenvalues using topology optimization, Struct. Multidisc. Optim., 20 (2000), pp. 2–11.
[31] L. Rudin, S. Osher, and E. Fatemi, Nonlinear total variation based noise removal algorithms, Phys. D, 60 (1992), pp. 259–268.
[32] M. Salahi and M. Ganji, A generalized newton-penalty algorithm for large scale ill-conditioned quadratic problems, Int. J. Appl. Math. Comp., 4 (2009), pp. 273–278.
[33] P. Schiavone and C. Ru, Solvability of boundary value problems in a theory of plane-strain elasticity with boundary reinforcement, Int. J. Eng. Sci., 47 (2009), pp. 1331–1338.
[34] X. Tai and H. Li, A piecewise constant level set method for elliptic inverse problems, Appl. Numer. Math., 57 (2007), pp. 686–696.
[35] A. Takezawa and M. Kitamura, Sensitivity analysis and optimization of vibration modes in continuum systems, J. Sound Vib., 332 (2013), pp. 1553–1566.
[36] D. Tcherniak, Topology optimization of resonating structures using SIMP method, Int. J. Numer. Meth. Eng., 54 (2002), pp. 1605–1622.
[37] The Mathworks Inc., Matlab User's Guide, Version 7, The Mathworks Inc., Natick, MA, 2004.
[38] B. P. Wang, Improved approximate methods for computing eigenvector derivatives in structural dynamics, AIAA J., 29 (1991), pp. 1018–1020.
[39] Z. Zhang and X. Cheng, A boundary piecewise constant level set method for boundary control of eigenvalue optimization problems, J. Comput. Phys., 230 (2011), pp. 458–473.
[40] Z. Zhang, K. Liang, and X. Cheng, A monotonic algorithm for eigenvalue optimization in shape design problems of multi-density inhomogeneous materials, Commun. Comput. Phys., 8 (2010), pp. 565–584.
[41] Z. Zhang, K. Liang, and X. Cheng, Greedy algorithms for eigenvalue optimization problems in shape design of two-density inhomogeneous materials, Int. J. Comput. Math., 88 (2011), pp. 183–195.
[42] H. Zhao, T. Chan, B. Merriman, and S. Osher, A variational level set approach to multiphase motion, J. Comput. Phys., 127 (1996), pp. 179–195.